# Implications of HBV-Driven Epigenetic Remodeling and Its Targets in Liver Cancer Stem Cells

**Ayse Banu Demir**
Izmir Ekonomi Universitesi Tıp Fakültesi
**Domenico Benvenuto**
Universita Campus Bio-Medico di Roma
**Bilge Karacicek**
Izmir Biyotıp ve Genom Merkezi
**Yasemin Erac**
Ege Universitesi
**Silvia Angeletti**
Universita Campus Bio-Medico di Roma
**Massimo Ciccozzi**
Universita Campus Bio-Medico di Roma
**Metiner Tosun** ( metiner.tosun@iue.edu.tr )
Izmir University of Economics, Faculty of Medicine https://orcid.org/0000-0002-2233-5720

**Research article**

**Keywords:** Hepatocellular carcinoma, HBx, miR3653, Epithelial-Mesenchymal transition (EMT), Molecular Evolution

**Posted Date:** July 21st, 2020

**DOI:** https://doi.org/10.21203/rs.3.rs-45377/v1

# Abstract

**Background:** Elevated levels of STIM1, an endoplasmic reticulum $Ca^{2+}$ sensor/buffering protein, appear to be correlated with poor cancer prognosis where microRNAs are also known to be involved. We investigated a possible viral origin of specific microRNAs identified in Huh-7 human liver cancer stem cells with enhanced STIM1 expression.

**Methods:** Computational strategies including phylogenetic analyses were performed on miRNome data obtained from Huh-7 liver cancer stem cells with enhanced STIM1 and/or Orai1 expression originally cultured in the present study.

**Results:** Results revealed two putative regions in HBV genome based on apparent clustering pattern of stem loop sequences of microRNAs, including miR3653. Reciprocal analysis of these regions revealed critical human genes of which their transcripts are among the predicted targets of miR3653 which was increased significantly by *STIM1* enhancement.

**Conclusion:** This study presents a phylogenetic evidence for an HBV-driven epigenetic remodeling to alter gene expression pattern associated with $Ca^{2+}$ homeostasis in STIM1-overexpressing liver cancer stem cells for a possible mutual survival outcome. A novel region on HBV-X protein may affect liver carcinogenesis in a genotype-dependent manner. Therefore, detection of the HBV genotype would have a clinical impact on prognosis.


# Background

Hepatitis B virus (HBV), a hepatotropic DNA virus with different genotypes, replicates via reverse transcriptase and incorporates into the host genome at early steps of clonal tumor expansion which eventually leads to hepatocellular carcinoma (HCC)[1–3]. In Huh-7 HCC cell lines, epithelial cell adhesion molecule (EpCAM)- and Prominin-1 (CD133)-expressing cell subpopulations were shown to possess cancer stem cell (CSC)-like properties as they frequently caused tumor development in mice xenograft models[4–6]. Enhancement of endoplasmic reticulum (ER) transmembrane stromal interaction molecule 1 (STIM1) and/or plasma membrane $Ca^{2+}$ channel (Orai1) expression in Huh-7 CSCs increased store-operated $Ca^{2+}$ entry (SOCE) and proliferation rate along with upregulated MDR1 expression, each associated with poor cancer prognosis[7].

SOCE-mediated increase in cytosolic $Ca^{2+}$ concentration appears to be among the initial events in HBV-associated hepatocarcinogenesis[8, 9]. HBxAg, an HBV-*X* gene-encoded protein with a wide spectrum of functions including viral life-cycle, is required for an effective infection and oncogenic potential[1]. HBx reportedly increases intracellular $Ca^{2+}$ levels via SOCE, stimulates cell proliferation and induces HBV replication in HCC[8, 10], Therefore, HBx could have essential roles in HBV-associated HCC by interacting with STIM1 and Orai1 complex to maintain SOCE, as well as targeting key microRNAs (miRNAs) in host cells[9, 11–14]. In viral infections, miRNAs can alter viral replication processes by regulating the viral gene

expression and cellular factors associated with HBV pathogenesis[15]. Many host miRNAs appear to be associated with HBV-induced genomic instability and their expression profile was altered in stable HBV-expression[16].

A possible causative role of STIM1 elevation in different types of cancer makes it an attractive chemotherapeutic target[14, 17]. Therefore, this study investigates a possible phylogenetic relationship between HBV and certain miRNAs whose expression patterns were altered by STIM1 and/or Orai1 enhancement in Huh-7 HCC CSCs. Our analyses revealed certain viral genomic segments either as a possible origin of some miRNAs critical for cancer cell survival or edited in order to activate host's epigenetic defense system on behalf of the virus.

# Methods

### Cell culture

Huh-7 HCC cell lines, originally from Dr. Jack Wands Laboratory (Massachusetts General Hospital, Boston, MA), were tested for authenticity via DNA profiling (Applied Biosystem's Identifier kit, PN 4322288), at DNA Sequencing & Analysis Shared Resource, University of Colorado Cancer Center. The cells' identity was reconfirmed by Idexx Bioresearch Company (Germany) before conducting present study. Mycoplasma contamination was monitored regularly in our laboratory by using MycoAlert Mycoplasma Detection Kit (Lonza). All cell culture processes were performed as described earlier[7].

### Separation of Huh-7 cancer stem cells

Cells were prepared for a fluorescence-activated cell sorter (FACS Aria III, BD Biosciences)[7]. Separation process was carried out based on differential fluorescence emission properties of labeled antibodies targeting EpCAM and CD133 (EpCAM-FITC, CD133-PE, Miltenyi). EpCAM- and/or CD133-expressing cells were collected separately in FBS-containing tubes. The percentages of EpCAM(+)/CD133(+) cell populations were recalculated by flow cytometry (FACSCalibur, BD Biosciences) on the same day.

### Plasmid transfection

Cells incubated for 24 hours with X-tremeGENE HP DNA Transfection Reagent (Roche) on 6 well-plates (105 cells/well) were transfected with plasmid DNA (MO70-STIM1-eYFP, pDEST501-Orai1-CFP and pCMV6 empty vector as control) for additional 1 hour[7]. Plasmids were kindly provided by Dr. M. Trebak (Penn State University).

### Invasion assay

48 hours after transfection, control and STIM1-OE and Orai1-OE Huh-7 HCC CSCs, were cultivated in 6-well plates (Corning, 8 µm-pore diameter, $6x10^4$ cell/well) to investigate invasion and migration characteristics. After 24 hours, cells were stained and migrating cells were counted under microscope.

## Data analyses

### PCR analyses for EMT markers

mRNA expression levels of target genes (E-cadherin, N-cadherin and Vimentin) were determined using qRT-PCR (LightCycler 1.5, Roche). cDNAs were synthesized (Transcriptor High Fidelity cDNA synthesis kit) by using RNA samples (1 µg) isolated from the cells (HighPure RNA Isolation Kit, Roche). FastStart DNA Master SYBR Green I Kit (Roche) was used to determine mRNA expression levels (Supplementary Table 4). Serial dilutions of standard 18S rRNA cDNA–containing plasmid with known copy number was used in each PCR run to construct linear regression curve to calculate mRNA concentrations specifically for each study as decribed earlier[7].

### miRNome analysis

Total RNA was extracted from cell samples using Total RNA Purification Kit (Norgen) which also allows collecting small non-coding RNAs including miRNAs, according to the manufacturer's instructions. RNA concentrations in each sample were determined by Nanodrop (Thermo Fischer Scientific). Isolated total RNA samples were analyzed (Agilent Bioanalyzer 2100) to calculate the "RNA Integrity Number" (RIN) (1 to 10) of which the value close to 10 shows robustness of the RNA content. Therefore, the samples with RIN ≥7were used in library preparation. A stepwise procedure was performed to prepare cDNA libraries from small RNA samples via ligation of 3 'and 5' adapters, excision of the corresponding constructs from the gel, purification and cDNA preparation via RT reaction, according to the manufacturer's instructions. Regarding the critical step in gel electrophoresis, the portion between the lower limit of the 160 bp band and the upper limit of the 145 bp band was recovered from the gel to collect the cDNAs of interest as the size of the original mature miRNAs is approximately 22 nt which reaches 147-150 nt with the addition of 3 'and 5' adapters.

Next generation sequencing (Illumina NextSeq 500), was performed (DONE Genetics & Bioinformatics, Istanbul, Turkey) on cDNA libraries prepared from total small RNA samples isolated in our laboratory. In Solexa sequencing method used by Illumina, DNA fragments were first placed on flow-cells and amplified locally to give high accuracy signal at the site of settlement (bridge-amplification). As a result, millions of clusters are formed on the flow-cell. Fragment clusters formed on the flow-cell were sequenced to read one base per cycle. In each cycle, DNA fragments were labeled with 4 different dyes and exposed to 4 different dinucleotides by the Sequencing-by-Synthesis method developed by Illumina. In each cycle, the clusters were visualized by fluorescence camera following binding of the appropriate dinucleotide. Images from each cluster were combined and the nucleotide sequences were deduced from the emission characteristics of the respective clusters.

Quality control: Efficiency of the sequencing process was assessed by using FASTQC program (www.bioinformatics.babraham.ac.uk). Reading filters and trimming: During the sequencing process, poor quality base readings in the FastQ readout data were excluded from readings to avoid false positive results in subsequent analysis steps. Trimmomatic application (http://www.usadellab.org/cms/ ?

Page=trimmomatic) was used for quality filters and trimming procedures. In order to detect miRNA sequences, the identified individual sequences were matched with BLAST via miRBase (www.mirbase.org). If the examined sequences match exactly the miRNA sequences in the miRBase, the corresponding sequence was considered as a miRNA candidate.

### RNA-Seq data analysis

NextSeq 500 (Illumina) sequencing data were generated in *.bcl format. These files contain the location and IDs of each DNA clusters on the flow cell and the emission characteristics. From these data, *.fastq files were obtained by using Bcl2fastq v.2.1 (Illumina) program. At the same time, fastq data were divided into different samples according to the index data (Demultiplexing).

### Phylogenetic analysis of miRNAs

Stem loop regions of the miRNAs, whose expression levels were significantly altered in CSCs due to STIM1 and/or Orai1 overexpression compared to their corresponding control Huh-7 cells, were retrieved from MirBase Database (http://www.mirbase.org/search.shtml). A dataset containing the stem loop sequences of 73 miRNAs has been built. In order to compare these sequences with HBV genome, the dataset have been constructed including these miRNAs and HBV genotypes A, B, C, D, E, F, G and H sequences. The sequences were aligned using MAFFT server (https://mafft.cbrc.jp/alignment/server/) and then manually edited by using Aliview software. Then, they were divided into sub datasets containing different DNA regions with the highest degree of sequence alignment and tentatively named as “Region 1” and “Region 2” for HBV. A Neighbor-joining tree (NJ), a Minimum Parsimony (MP), a Bayesian Phylogenetic Tree (BP), Minimum Evolution Tree (ME) and a minimum spanning tree (MST) based on the Kruskal genetic distance plot were drawn for each region using MEGA-7 software for ME, NJ and MP; Mr. Bayes for the BP and an in-house script in R for MST. Pairwise *genetic distances* were calculated by *MEGA* software (version *7.0*). The trees were compared and discussed based on the miRseq data obtained from Huh-7 HCC stem cells. Unresolved trees were discarded and miRNAs that changed upon plasmid-only transfection were excluded from further analysis.

The HBx regions aligned with some parts of the stem-loop sequences were analyzed separately due to the presence of numerous nucleotide mismatches. The resolved trees (MST and ME) were performed independently for distinct regions and only miRNAs clustered close to the viral genome in both approaches were evaluated. Due to sequence shortness, clusters emerged by two different mathematical models were used to confirm the similarity between the human miRNAs and the putative regions of HBV genome.

### Genomic database analysis

HBV Regions 1 and 2 were compared with the HBV genome (https://hbvdb.ibcp.fr/HBVdb/HBVdbGenome) in order to identify with which genetic region in the HBV genome they overlap and further BLAT alignment algorithm was used to identify a possible region within

the human genome (hCG38) in which these regions are aligned (http://genome.ucsc.edu/cgi-bin/hgBlat). BLAT analysis was performed instead of BLAST since the sequences were too short for BLAST analysis.

### Putative protein structure homology analysis

The protein file for HBx was downloaded from SWISS-MODEL (https://swissmodel.expasy.org/repository/uniprot/Q156X2). The putative “Region 1” (amino acids between 10 and 34) and “Region 2” (amino acids between 117 and138) on HBx protein were labeled by using RasMol program for Windows (RasWin). In order to find protein structures similar to the identified HBV regions, homologous structural templates have been searched and validated using the template search tools HHpred[18] and SwissModel[19]. Three dimensional structures have been constructed by using PyMOL (The PyMOL Molecular Graphics System, Version 2.0 Schroedinger, LLC). The QMEAN Z Score and GMQE (Global Model Quality Estimation) have been used to calculate the degree of nativeness of the structural feature observed in the model on a global scale and to estimate the quality of the 3D model, respectively[20].

### Statistics

PCR and invasion assay data are expressed as mean ± standard error of the mean. “n” represents the number of samples. Statistical significance between the means of two groups was evaluated using Student’s *t*-test (unpaired data) using Graph Pad

Prism software (GraphPad, San Diego CA, USA) and $P<0.05$ considered statistically significant.

## Results

### miRNA profile upon *Orai1* and *STIM1* overexpression

Based on our miRNome data, enhancement of STIM1 and/or Orai1, which mimic poor HCC prognosis, significantly altered expression levels of 73 miRNAs in Huh-7 CSCs (Supplementary Table 1). miR3653 and miR5001 were the only miRNAs that were significantly upregulated (Fold Change[FC]>1.5, in red) in all CSC samples (Fig. 1).

### Phylogenetic analysis of miRNAs

Stem loop sequences of the miRNAs that were significantly altered upon STIM1 and/or Orai1-enhancement, were used in phylogenetic analyses to quest their viral origin. Multiple alignment analyses revealed two putative HBV segments, "Region 1” and “Region 2” (Fig. 2, Supplementary Table 2), where most of the stem-loop sequences were aligned.

Due to presence of many unmatched nucleotides between these two regions, further phylogenetic analyses were performed separately for each region. Among all phylogenetic analyses, only minimum evolution (ME) and minimum spanning tree (MST) were able to draw resolved trees, whereas

Neighbourhood Joining (NJ), Maximum Parsimony (MP) and Bayesian Parsimony (BP) algorithms were not operational. Therefore, stem loop sequences of miRNAs clustered close to HBV genotypes in both trees were analyzed further.

miR3150a and miR3653 clustered close to HBV "Region 1" in both trees (Fig. 3A and Fig. 3B). miR3150a(5p) was downregulated in CSCs compared to that of parental HCC cells, while miR3653(3p) upregulated in both *STIM1*-and/or *Orai1*- overepressing CSCs compared to that of control CSCs (Fig. 3C).

Regarding the miRNAs clustered within HBV "Region 2" (Fig. 4); miR125b-1(3p) was downregulated in CSCs compared to parental HCC cells, while miR3194(5p) was upregulated.

### Genomic database analysis of putative HBV regions

The identified HBV regions were used in BLAT analysis against the human genome (hCG38) (http://genome.ucsc.edu/cgi-bin/hgBlat). Although HBV "Region 1" did not match the human genome, "Region 2" showed several matching regions in a genotype-dependent manner (Supplementary Table 3).

### Structural homology analysis

Locations of "Region 1" and "Region 2" on HBx protein were shown in Fig. 5A. For homology analysis, these regions within all different HBV genotypes were used as separate reference sequences to investigate if any homology exists with human proteins. Homologies were primarily identified for genotype F (DQ823095). The calculated QMEAN z Score was statistically significant (-4<QMEAN z Score<0) and the GMQE (Global Model Quality Estimation) score that is used to estimate the quality of the three-dimensional model was 0.4, considered an average for heterodimeric models constructed by short sequences according to the software algorithm guidelines. These results showed the convenience of the model for our purpose. Among all HBV genotypes tested, homology models were found only for "Region 2" templates. These models yielded two candidate proteins; membrane-associated guanylate kinases p55 subfamily member 7 (MPP7) (PDB code 3lra.1.A), for HBV genotypes A, B, E, G and H (Fig. 5B) and Latent Transforming Growth Factor β Binding Protein 1 (TGF β-LTBP-1) (PDB code 1ksq.1.A), for HBV genotypes C, D and F (Fig. 5C).

### E-Cadherin expression changes

In order to test the effects of STIM1- and/or Orai1-enhancement in Huh-7 HCC CSCs, on "Epithelial to Mesenchymal Transition (EMT)" and "Mesenchymal to Epithelial Transition (MET)", transcription levels of epithelial (E-cadherin) and mesenchymal (N-cadherin and vimentin) markers, were determined. E-cadherin expression was significantly increased both by *STIM1*- and *STIM1* plus *Orai1*-enhancement (Fig. 6) while no significant change was observed in N-cadherin and vimentin (not shown).

# Discussion

In order to partially reveal the molecular events behind HCC poor prognosis, *STIM1* and/or *Orai1* expression were enhanced *in vitro* in EpCAM- and CD133-expressing Huh-7 CSC subpopulation and the miRNA profile was evaluated based on extensive NGS miRNome data. miRNAs, whose expressions significantly altered upon enhancement of *STIM1* and/or *Orai1*, were further used in phylogenetic analyses to quest their viral origin. Multiple alignment results of the stem loop nucleotide sequences of these small non-coding RNAs revealed two putative HBV segments, as we proposed "Region 1" and "Region 2", where most of these sequences were partially clustered in the HBx-region of HBV genome.

Previously, miR3653 expression levels were shown to be significantly lower in HCC cells compared to that of non-cancerous hepatocytes and its overexpression was shown to inhibit growth and metastatic ability of HCC cells[21]. This appears to mimic the dormant state of CSCs. In our study, besides being significantly upregulated by enhancement of *STIM1* and/or *Orai1* in CSCs, miR3653 was the only miRNA whose stem-loop sequence clustered within both "Region 1" and "Region 2". In addition, its predicted targets have essential roles in carcinogenesis (http://www.targetscan.org/cgi-bin/targetscan/vert_71/targetscan.cgi?mirg=has -miR-3653-3p). Approximately 20-22 nt-segment of viral Region 2 was found within the intronic regions of some of these target genes (Supplementary Table 3). Cellular roles of six significant targets were discussed below in terms of HBV virulence and carcinogenesis.

**Calpains (*CAPN*s):**

Calpains are family of $Ca^{2+}$-activated nonlysosomal intracellular cysteine proteases that cleave STIM1[22]. STIM1 and SOCE are linked to angiogenesis and cancer cell survival, both indicating tumor aggressiveness and poor prognosis[23]. Suppression of calpain by upregulated miR3653 in STIM1-enhanced HCC CSCs may have an additional survival outcome for the host.

**Carboxylesterase 4A (*CES4A):***

Certain parts of "Region 2" of HBV genotype A and F were found within the intronic region of *CES4A*. Carboxylases encoded by this gene are responsible for transesterification of certain endogeneous substrates and detoxification of various xenobiotics and drugs (https://www.genecards.org/cgi-bin/carddisp.pl?gene=CES4A). This gene was shown to be hypermethylated in HCC tissues[24]. Upregulation of miR3653(3p) in STIM1- and/or Orai1-overexpressing CSCs may suggest an additional epigenetic regulation of this enzyme in HCC. Hypermethylation of this gene and its posttranscriptional suppression by miR3653 can make cells vulnerable to xenobiotics. This dual epigenetic control could be a partial removal of the host defense system on behalf of the invading organism.

**Centrosomal protein 76 kDa *(CEP76)*:**

Being critical for many cellular processes, centriole numbers are strictly controlled since increase in their copy number is considered among the hallmarks of cancer[25]. *CEP76* appears to suppress centriole amplification suggesting that elevated miR3653 may contribute to the dormancy of liver CSCs via *CEP76*.

**Mucin 20 cell surface associated (*MUC20*):**

Overexpression of *MUC20*, which is considered as a prognostic marker in renal cancers (https://www.proteinatlas.org/ENSG00000176945-MUC20), involved in uncontrolled metastasis of colorectal cancer as well[26]. Some mucins also shown to be operational in primary liver lesions and HCC[27]. Integration of a certain segment of HBV genotype C in intronic regions of *MUC20* and upregulation of miR3653 targeting *MUC20* may make HBV-induced carcinogenesis liver resident, which is quite consistent with the hepatotropic property of the virus. This may explain why HCC does not metastasize extrahepatic tissues until advanced intrahepatic tumor stage IVA[28].

**Beta-1,4-N-acetyl-galactosaminyl transferase 3 (*B4GALNT3*):**

Certain parts of "Region 2" of HBV genotype D were found within the intronic region of *B4GALNT3,* which was shown to be overexpressed in colon cancer cells regulating the stemness[29]. Knock-down of *B4GALNT3* led to suppression of malignant phenotype[29]. Upregulation of miR3653(3p) in STIM1- and/or Orai1-overexpressing CSCs may, therefore, be a host defense response against the malignancy. This integration appears to be a part of the evolutionarily-triggered survival strategy of human cells hosting HBV.

**Mitochondrial $Ca^{2+}$ uniporter (MCU):**

MCU, a transmembrane protein that allows $Ca^{2+}$ uptake into mitochondria, and its regulatory components *MICU1* and *MICU2* are among the targets of miR3653. Upregulation of miR3653 by *STIM1*-enhancement may account for survival of the CSCs by precluding $Ca^{2+}$-induced apoptosis carried out by mitochondria. On one hand, overexpression of STIM1 increases $Ca^{2+}$ storage capacity of ER, on the orther hand, miR3653 guarantees CSC survival. Consistent with the other miR3653 targets discussed above; downregulation of MCU also appears to be a part of the survival strategy of the host cells.

Upon BLAT analysis of the identified HBV regions against human reference genome, Region 2 was found in intronic regions of several human genes while Region 1 was not. Evaluation of 192 DNA sequences from tumor and corresponding non-tumor samples revealed direct repeat region (DR1), the most common fusion breakpoint of HBV genome[30]. Integration of the HBV "Region 2" into human genome, unlike "Region 1", may result from its close proximity to DR1.

Both Region-1 and Region-2 reside within the HBx-encoding region of HBV (https://hbvdb.ibcp.fr/HBVdb/HBVdbGenome). Previously, different parts of HBx protein were shown to behave differently to chemotherapy, indicating the possibility of designated roles for specific parts of HBx[31]. Based on this information, the putative HBV "Region 2" (amino acids 117 to 138), may have functional impact on HCC development through genetic or epigenetic mechanisms. Moreover, "Region 2", is an overlapping region for HBx (nt. 1374-1835), HBV core promoter (nt. 1611-1647) and Enhancer II (nt. 1685-1742), as well as a binding site for several transcription factors including HNF3, HNF4, TBP, Sp1[32, 33], regulators of viral transcription[34]. This region also seems to be a hotspot for high-risk HCC

mutations[32] having clinical impact on chronic HBV and HCC[33]. Therefore, investigation of the regulatory roles of this region both in HBV and human genome could have translational value.

A high sequence homology of “Region 2” in different HBV genotypes with different intronic regions in human genome is a serendipitous finding of this study. Although HBV integration known to occur randomly throughout the entire human genome, it may also show some genotype-dependent pattern[35, 36]. Besides well-defined preferred integration regions[37], viral insertion preference into variable locations in host genome through this specific HBx region for different HBV genotypes is a novel observation.

In our *in silico* analysis, the putative “Region 2” was also found in intronic regions of *CASC8*, *SLC32A1* and *RPL23AP5*, which were previously shown to harbor integrated HBV genome sections in HCC patients[35]. Therefore, extended analysis of the targets identified in this study in human samples may reveal a function of Region 2 in HCC prognosis. Integration of different HBx mutants into host genome was reported to be responsible for altered carcinogenesis in different patients[38]. Based on our data, we further suggest that patient specific prognosis may also depend on this variable genomic integration.

Based on homology analysis, certain parts of two proteins, Mpp7 and TGF β-LTBP, which affect EMT processes, were revealed to share high homology with Region 2. Mpp7 plays role in formation of tight junctions between epithelial and endothelial cells, which are crucial for cancer progression and metastasis[39–41], as well as in establishment and maintenance of apicobasal polarity in epithelial tissues. Altered apicobasal polarity, which normally inhibits epithelial to mesenchymal transformation (EMT) to suppress metastasis[42], is one of the initial modifications observed during carcinogenic transformation[43]. EMT, which is crucial for tumor progression, requires loss of cell to cell contacts and apical-basal polarity of epithelial cells[44, 45]. The homology of “Region 2” of some HBV genotypes to Mpp7p suggested a possible involvement of this region in apicobasal polarity.

TGF-β has dual effects on HCC cancer cells by both suppressing or stimulating tumor development[11]. Inhibition of TGF-β signaling reduces the synthesis and release of connective tissue growth factor in tumor environment, which suppresses tumor cell growth, intravasation, and metastatic dissemination[46, 47]. Serum levels of TGFβ-LTBP-1 measured in a cohort of Anti-HCV/HBsAg demonstrated a gradual increase in healthy individuals eventually developing liver cirrhosis and HCC[48]. EMT and enhancement of cell migration and invasion along with differential effects of STIM1 on TGFβ-induced EMT, appear to be correlated with elevated $Ca^{2+}$ influx via SOCE as shown in breast cancer cells[49]. Along with increased proliferation rate as observed in our previous study[7], STIM1- and/or Orai1-overexpressed HCC CSCs appeared to be in an interim state favoring epithelial transition (MET). Significant elevation in epithelial marker E-cadherin along with upregulated mesenchymal markers (N-Cadherin and vimentin), presenting a partial EMT behavior, suggested that STIM1 and/ Orai1-enhancement leads CSCs into second phase (equilibrium) of 3Es (Elimination, Equilibrium and Escape) of cancer immunoediting process fascilitating a shift from EMT to MET depending on the microenvironment[50]. Significantly upregulated SOCE-related cytosolic $Ca^{2+}$ levels[7] appeared to be responsible for the enhanced invasion pattern of *STIM1*- and *Orai1*-enhanced CSCs, as *STIM1*-enhancement, *per se,* inhibited invasion drastically.

*In silico* determination of “Region 2” for being highly homologous to certain regions in TGFβ-LTBP-1 and Mpp7p, and its integration into the human genome suggest that HBV indirectly affects EMT via two different pathways in order to promote liver cancer progression in a genotype-dependent manner. Therefore, identification of the HBV genotype in infections may reveal how EMT is regulated in HCC progression. Upregulation of epithelial marker, E-cadherin, upon *STIM1* and/or Orai1 enhancement, emphasizes the impact of miR3653 along with Mpp7 and TGFβ-LTBP on EMT process which awaits further investigation of human gene targets where HBV Region 2 is integrated.

The miRNA expression pattern of CSCs upon mimicking poor prognosis *in vitro* and partial integration of “Region 2” in different intronic regions of human genome in various HBV genotypes along with protein homologies *in silico* raises the question whether each HBV genotype follows a different epigenetic strategy in carcinogenesis.

miR3653 appears to be a part of the host defense mechanism recognized by HBV as its stem loop sequence remnants are found in viral HBx region. This mechanism may be mutually favorable for both viral replication process and the host until the terminal stage of HCC. STIM1 upregulation favors host cell survival by upregulating miR3653 which suppresses both calpain and MCU, further guaranteeing uninterrupted cycle of protein machinery in the HBV-infected host cell (Fig. 7). Furthermore, having this versatile genetic repertoire, HBx appears to be a “master key” in virulence as well as virus-driven epigenetic regulation of hepatocarcinogenesis.

# Conclusion

Together, our phylogenetic analyses suggest that a possible “survival strategy” of HBV-induced liver CSCs might have been developed throughout the evolution as HBV “Region 2” remnants were found in human genome. Lacking similar DNA stretches in antique (possibly 40-million-years-old) HBV might prove this genetic mimicry which disguises foe as friend. The presence of critical mRNAs coding for proapoptotic proteins among the targets of specific miRNAs found in our study suggest that the virus might have developed a highly sophisticated survival toolbox in HBx region possibly via genome editing acquired throughout the long-lasting interaction with human cells. As University of Queensland virologist Paul Young quoted earlier “The boundaries between organisms are a bit more merged now, a bit more shadowy. We need to break down those boundaries. The more we look, the more we find overlap.” (https://www.pbs.org/wgbh/nova/article/endogenous-retroviruses/, accession date: Nov.23, 2019).

# Abbreviations

HBV: Hepatitis B virus; HCC: Hepatocellular carcinoma; EpCAM: Epithelial cell adhesion molecule; CD133: Prominin-1; CSC: Cancer stem cell; STIM1: Endoplasmic reticulum (ER) transmembrane stromal interaction molecule 1; Orai1: Plasma membrane $Ca^{2+}$ channel; SOCE: Store-operated $Ca^{2+}$ entry; miRNA: micro RNA; Mpp7: Membrane-associated guanylate kinases p55 subfamily member 7; TGFβ -LTBP1:

Latent Transforming Growth Factor β-Binding Protein 1; EMT: Epithelial to mesenchymal transition; MET: Mesenchymal to epithelial transition; DR1: Direct repeat region 1

# Declarations


### Acknowledgements

Authors acknowledge Dr. M. Trebak (Dept. of Cellular and Molecular Physiology, Penn State Cancer Institute, Hershey, PA, USA) and Dr. X. Hu (IBG Izmir) for providing plasmid vectors and technical support in cell sorting, respectively. miRNA deep sequencing data obtained from Huh-7 CSCs used for the bioinformatic analyses were performed by DONE Genetics and Bioinformatics Inc. (Istanbul, Turkey).

### Funding

This study was funded by the Scientific and Technological Research Council of Turkey (TUBITAK Project# 113S399 to M.T.).


### Availability of data and materials

The datasets are available as supplementary file.

### Authors' contributions

MT and ABD conceived the study. MT and YE designed, analyzed and interpreted the functional studies. BK performed cell culture studies, transfections and prepared DNA libraries for miRNome studies. ABD and DB designed and performed all computational strategies including phylogenetic analyses supervised by MC. ABD and MT interpreted miRNome data. ABD and MT wrote the draft manuscript. DB, SA and MC provided critical review of the manuscript. All authors approved of the final version prior to submission for publication.

### Consent for publication

Not applicable.

### Competing interests

The authors declare that they have no competing interests.

### Author details


[1] Dept. of Medical Biology, School of Medicine, Izmir University of Economics, 35330, Izmir, Turkey, banu.demir@ieu.edu.tr

[2] Faculty of Medicine, University Campus Bio-Medico of Rome (UCBM), Rome, Italy, domenicobenvenuto95@gmail.com

[3] Izmir Biomedicine and Genome Center (IBG), Dokuz Eylul University Health Campus, Izmir, Turkey, bilge.karacicek@ibg.edu.tr

[4] Dept. of Pharmacology, Faculty of Pharmacy, Ege University, 35100 Izmir, Turkey, yasemin.erac@ege.edu.tr

[5] Clinical Laboratory Science Unit, Faculty of Medicine, University Campus Bio-Medico of Rome (UCBM), Rome, Italy, s.angeletti@unicampus.it

[6] Medical Statistics and Molecular Epidemiology Unit, Faculty of Medicine, University Campus Bio-Medico of Rome (UCBM), Rome, Italy, m.ciccozzi@unicampus.it

[7] Dept. of Medical Pharmacology, School of Medicine, Izmir University of Economics, 35330, Izmir, Turkey, metiner.tosun@ieu.edu.tr

*Correspondence: metiner.tosun@ieu.edu.tr, Tel: +90(232) 488 9843, Fax: +90(232) 279 2626

# References

1. Liang TJ. Hepatitis B: The virus and disease. Hepatology. 2009;49.
2. Tu T, Budzinska MA, Shackel NA, Urban S. HBV DNA integration: Molecular mechanisms and clinical implications. Viruses. 2017;9(4):75.
3. Shi W, Zhang Z, Ling C, Zheng W, Zhu C, Carr MJ, et al. Hepatitis B virus subgenotyping: History, effects of recombination, misclassifications, and corrections. Infection, Genetics and Evolution. 2013.
4. Lee TKW, Cheung VCH, Ng IOL. Liver tumor-initiating cells as a therapeutic target for hepatocellular carcinoma. Cancer Letters. 2013; 338(1):101-109.
5. Liu R, Shen Y, Nan K, Mi B, Wu T, Guo J, et al. Association between expression of cancer stem cell markers and poor differentiation of hepatocellular carcinoma: A meta-analysis (PRISMA). Med (United States). 2015;94(31):e1306.
6. Chen Y, Yu D, Zhang H, He H, Zhang C, Zhao W, et al. CD133+EpCAM+ phenotype possesses more characteristics of tumor initiating cells in hepatocellular carcinoma Huh7 Cells. Int J Biol Sci. 2012; 8(7):992-1004.
7. Karacicek B, Erac Y, Tosun M. Functional consequences of enhanced expression of STIM1 and Orai1 in Huh-7 hepatocellular carcinoma tumor-initiating cells. BMC Cancer. 2019;19(1):751.
8. Yang B, Bouchard MJ. The Hepatitis B Virus X Protein Elevates Cytosolic Calcium Signals by Modulating Mitochondrial Calcium Uptake. J Virol. 2012;86(1):313-327.
9. Yao J hong, Liu Z jian, Yi J hua, Wang J, Liu Y nan. Hepatitis B Virus X Protein Upregulates Intracellular Calcium Signaling by Binding C-terminal of Orail Protein. Curr Med Sci. 2018;38:26-34.

10. Choi Y, Gyoo Park S, Yoo JH, Jung G. Calcium ions affect the hepatitis B virus core assembly. Virology. 2005; 332(1):454-463.
11. Murata M, Matsuzaki K, Yoshida K, Sekimoto G, Tahashi Y, Mori S, et al. Hepatitis B virus X protein shifts human hepatic transforming growth factor (TGF)-β signaling from tumor suppression to oncogenesis in early chronic hepatitis B. Hepatology. 2009;49(4):1203-1217.
12. Paterlini-Bréchot P, Saigo K, Murakami Y, Chami M, Gozuacik D, Mugnier C, et al. Hepatitis B virus-related insertional mutagenesis occurs frequently in human liver cancers and recurrently targets human telomerase gene. Oncogene. 2003;22:3911-3916.
13. Wang Z, Wu Z, Huang P. The function of miRNAs in hepatocarcinogenesis induced by hepatitis B virus X protein (Review). Oncology Reports. 2017;38(2):652-664.
14. Yang Z, Li J, Feng G, Wang Y, Yang G, Liu Y, et al. Hepatitis B virus X protein enhances hepatocarcinogenesis by depressing the targeting of NUSAP1 mRNA by miR-18b. Cancer Biol Med. 2019;16(2):276-287.
15. Skalsky RL, Cullen BR. Viruses, microRNAs, and Host Interactions. Annu Rev Microbiol. 2010;64:123-141.
16. Liu Y, Zhao JJ, Wang CM, Li MY, Han P, Wang L, et al. Altered expression profiles of microRNAs in a stable hepatitis B virus-expressing cell line. Chin Med J (Engl). 2009;122(1):10-14.
17. Wang J, Shen J, Zhao K, Hu J, Dong J, Sun J. STIM1 overexpression in hypoxia microenvironment contributes to pancreatic carcinoma progression. Cancer Biol Med. 2019;16(1):100-108.
18. Zimmermann L, Stephens A, Nam SZ, Rau D, Kübler J, Lozajic M, et al. A Completely Reimplemented MPI Bioinformatics Toolkit with a New HHpred Server at its Core. J Mol Biol. 2018;430 (15):2237-2243.
19. Waterhouse A, Bertoni M, Bienert S, Studer G, Tauriello G, Gumienny R, et al. SWISS-MODEL: Homology modelling of protein structures and complexes. Nucleic Acids Res. 2018;46(W1):W296-W303.
20. Benkert P, Biasini M, Schwede T. Toward the estimation of the absolute quality of individual protein structure models. Bioinformatics. 2011;27(3):343-350.
21. Zhang L, Zhang T, Deng Z, Sun L. MicroRNA-3653 inhibits the growth and metastasis of hepatocellular carcinoma by inhibiting ITGB1. Oncol Rep. 2019;41(3):1669-1677.
22. Prins D, Michalak M. STIM1 is cleaved by calpain. FEBS Lett. 2015;589(21):3294-3301.
23. Yang Y, Jiang Z, Wang B, Chang L, Liu J, Zhang L, et al. Expression of STIM1 is associated with tumor aggressiveness and poor prognosis in breast cancer. Pathol Res Pract. 2017;213(9):1043-1047.
24. Udali S, Guarini P, Ruzzenente A, Ferrarini A, Guglielmi A, Lotto V, et al. DNA methylation and gene expression profiles show novel regulatory pathways in hepatocellular carcinoma. Clin Epigenetics. 2015;7(1):43.

25. Barbelanne M, Chiu A, Qian J, Tsang WY. Opposing post-translational modifications regulate Cep76 function to suppress centriole amplification. Oncogene. 2016;35(41):5377-5387.
26. Xiao X, Wang L, Wei P, Chi Y, Li D, Wang Q, et al. Role of MUC20 overexpression as a predictor of recurrence and poor outcome in colorectal cancer. J Transl Med. 2013;11:151.
27. Kasprzak A, Adamek A. Mucins: The old, the new and the promising factors in hepatobiliary carcinogenesis. International Journal of Molecular Sciences. 2019;20(6):1288.
28. Katyal S, Oliver JH, Peterson MS, Ferris J V., Carr BS, Baron RL. Extrahepatic metastases of hepatocellular carcinoma. Radiology. 2000;216(3):698-703.
29. Che MI, Huang J, Hung JS, Lin YC, Huang MJ, Lai HS, et al. β1, 4-N-acetylgalactosaminyltransferase III modulates cancer stemness through EGFR signaling pathway in colon cancer cells. Oncotarget. 2014;5(11):3673-3684.
30. Podlaha O, Wu G, Downie B, Ramamurthy R, Gaggar A, Subramanian M, et al. Genomic modeling of hepatitis B virus integration frequency in the human genome. PLoS One. 2019;14(7):e0220376.
31. Chau DK fan, Chen GG, Zhang H, Leung BCS, Chun S, Lai PB san. Differential Functions of C- and N-Terminal Hepatitis B x Protein in Liver Cells Treated with Doxorubicin in Normoxic or Hypoxic Condition. PLoS One. 2012;7(11):e50118.
32. Meier-Stephenson V, Bremner WTR, Dalton CS, van Marle G, Coffin CS, Patel TR. Comprehensive Analysis of Hepatitis B Virus Promoter Region Mutations. Viruses. 2018;10(11):603.
33. Quarleri J. Core promoter: A critical region where the hepatitis B virus makes decisions. World Journal of Gastroenterology. 2014;20(2):425-435.
34. Yu X, Mertz JE. Promoters for synthesis of the pre-C and pregenomic mRNAs of human hepatitis B virus are genetically distinct and differentially regulated. J Virol. 1996;70(12):8719-8726.
35. Zhao LH, Liu X, Yan HX, Li WY, Zeng X, Yang Y, et al. Genomic and oncogenic preference of HBV integration in hepatocellular carcinoma. Nat Commun. 2016;7:12992.
36. Furuta M, Tanaka H, Shiraishi Y, Unida T, Imamura M, Fujimoto A, et al. Characterization of HBV integration patterns and timing in liver cancer and HBV-infected livers. Oncotarget. 2018;9(38):25075-25088.
37. Budzinska MA, Shackel NA, Urban S, Tu T. Cellular genomic sites of hepatitis B virus DNA integration. Genes. 2018;9(7):365.
38. Huo TI, Wang XW, Forgues M, Wu CG, Spillare EA, Giannini C, et al. Hepatitis B virus X mutants derived from human hepatocellular carcinoma retain the ability to abrogate p53-induced apoptosis. Oncogene. 2001;20(28):3620-3628.
39. Martin TA, Watkins G, Mansel RE, Jiang WG. Loss of tight junction plaque molecules in breast cancer tissues is associated with a poor prognosis in patients with breast cancer. Eur J Cancer. 2004;40(17):2717-2725.
40. Martin TA, Jiang WG. Loss of tight junction barrier function and its role in cancer metastasis. Biochimica et Biophysica Acta - Biomembranes. 2009;1788(4):872-891.

41. Stucke VM, Timmerman E, Vandekerckhove J, Gevaert K, Hall A. The MAGUK protein MPP7 binds to the polarity protein hDlg1 and facilitates epithelial tight junction formation. Mol Biol Cell. 2007;18(5):1744-1755.
42. Jung HY, Fattet L, Tsai JH, Kajimoto T, Chang Q, Newton AC, et al. Apical–basal polarity inhibits epithelial–mesenchymal transition and tumour metastasis by PAR-complex-mediated SNAI1 degradation. Nat Cell Biol. 2019;21(3):359-371.
43. Treyer A, Müsch A. Hepatocyte polarity. Compr Physiol. 2013;3(1):243-287.
44. Spaderna S, Schmalhofer O, Wahlbuhl M, Dimmler A, Bauer K, Sultan A, et al. The transcriptional repressor ZEB1 promotes metastasis and loss of cell polarity in cancer. Cancer Res. 2008;68(2):537-544.
45. Moreno-Bueno G, Portillo F, Cano A. Transcriptional regulation of cell polarity in EMT and cancer. Oncogene. 2008;27(55):6958-6969.
46. Fransvea E, Angelotti U, Antonaci S, Giannelli G. Blocking transforming growth factor-beta up-regulates E-cadherin and reduces migration and invasion of hepatocellular carcinoma cells. Hepatology. 2008;47(5):1557-1566.
47. Fransvea E, Mazzocca A, Antonaci S, Giannelli G. Targeting transforming growth factor (TGF)-βRI inhibits activation of β1 integrin and blocks vascular invasion in hepatocellular carcinoma. Hepatology. 2009,49(3):839-850.
48. Aarag B El, Saad H, Hendy O, Samiee MA, Zahran M. Latent Transforming Growth Factor-beta Binding Protein-1 as a Diagnostic Biomarker for the Detection of Hepatocellular Carcinoma. J Mol Biomark Diagn. 2018;9(2):388.
49. Zhang S, Miao Y, Zheng X, Gong Y, Zhang J, Zou F, et al. STIM1 and STIM2 differently regulate endogenous Ca2+ entry and promote TGF-β-induced EMT in breast cancer cells. Biochem Biophys Res Commun. 2017;488(1):74-80.
50. Dunn GP, Old LJ, Schreiber RD. The Three Es of Cancer Immunoediting. Annu Rev Immunol. 2004;22:329-360.

# Figures

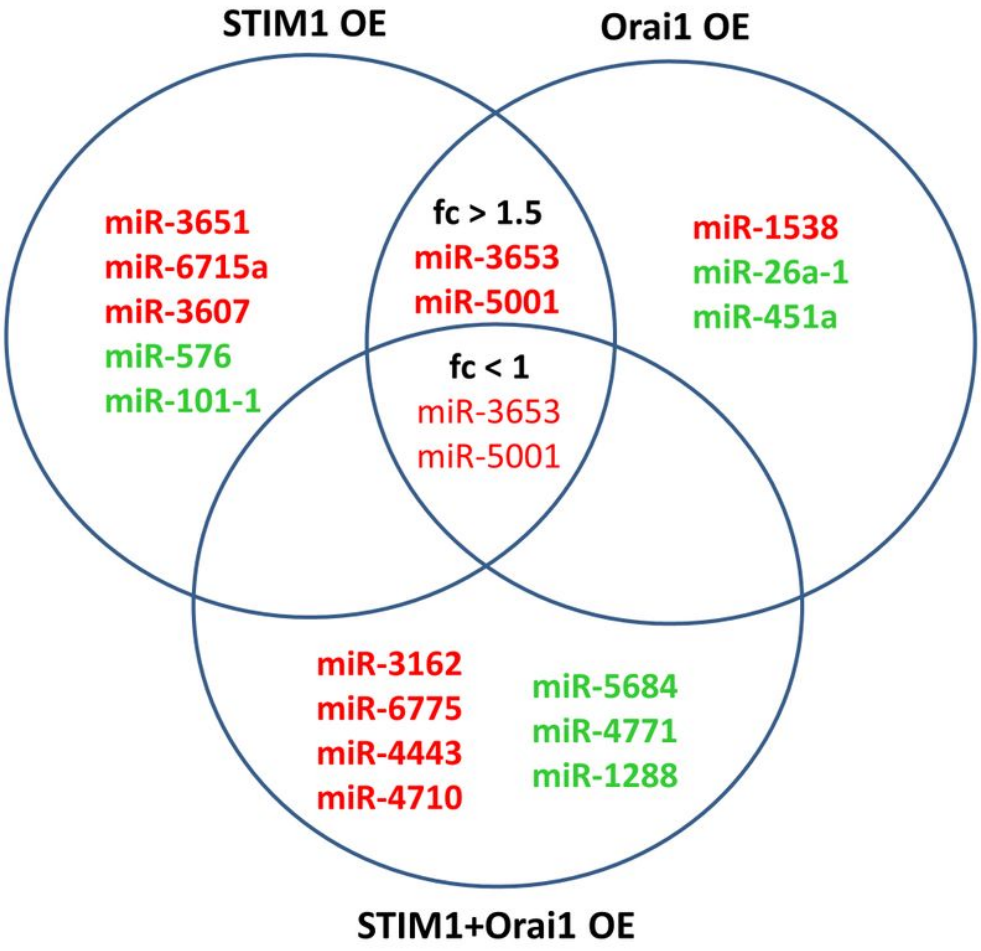


## Figure 1

Venn diagram showing candidate miRNAs with significantly altered expression levels. miRSeq data (Illumina NextSeq 500) were obtained from cancer stem cell samples treated with overexpression constructs for STIM1, Orai1 and STIM1&Orai1 enhancement. Upregulated and downregulated miRNAs are shown in red and green letters, respectively.

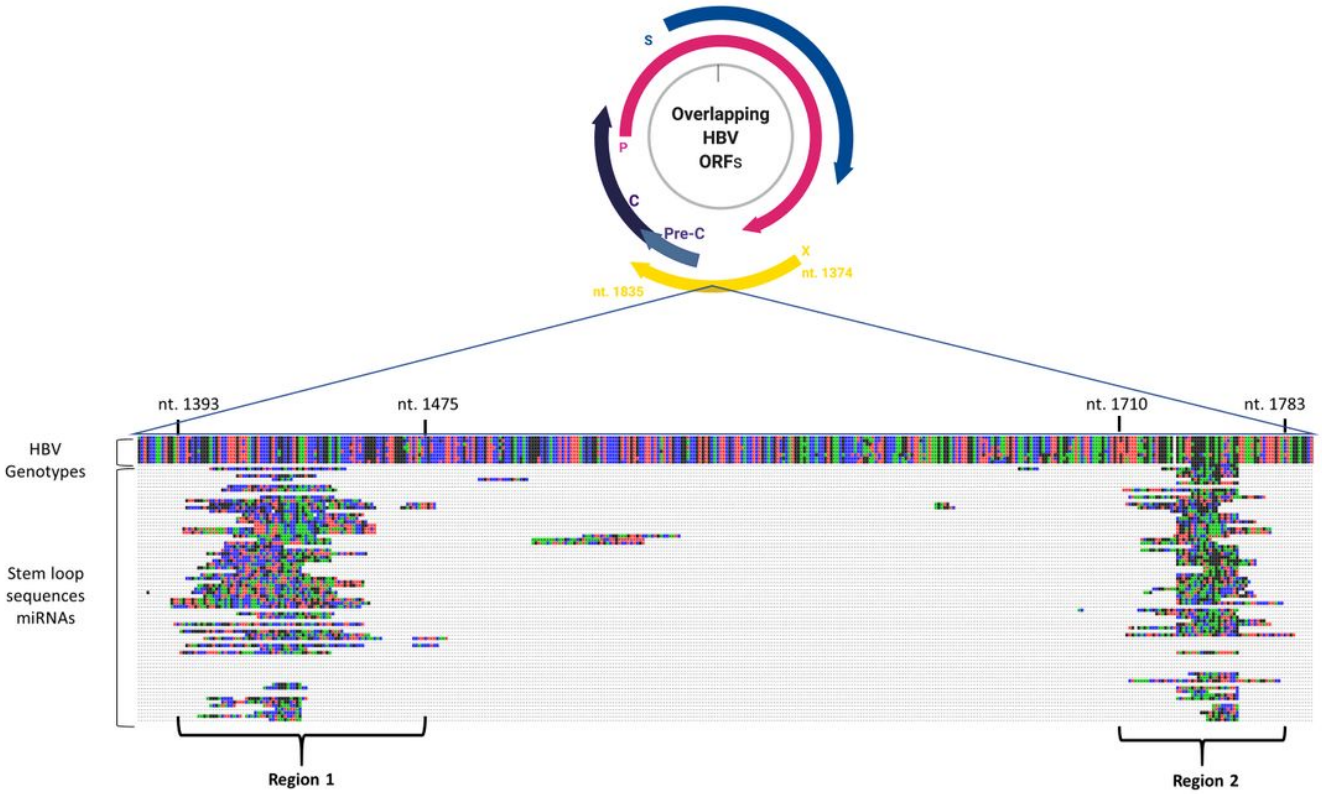


## Figure 2

Representation of HBV genome along with overlapping HBV Open Reading Frames (ORFs). The locations of “Region 1” (from HBV nucleotide 1393 to 1475) and “Region 2” (from HBV nucleotide 1710 to 1783) are shown on HBx coding region (from HBV nucleotide 1374 to 1835), where stem-loop sequences of many miRNAs are partially aligned through multiple sequence alignment. Only the stem-loop sequences of miRNAs were aligned to match HBV genome as no direct alignment pattern were found for their corresponding mature miRNAs.

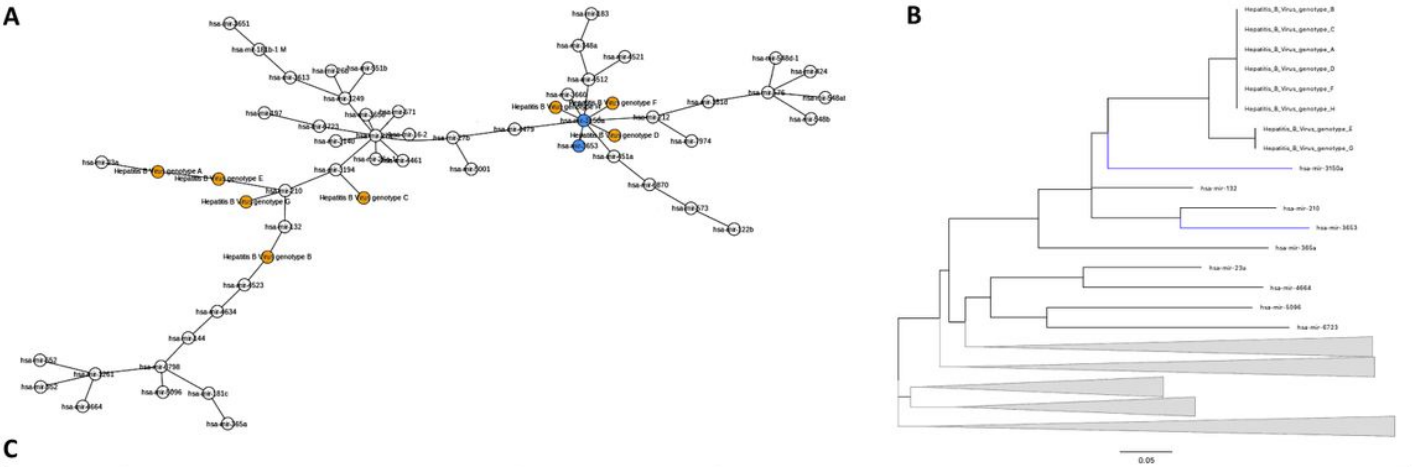


C

| miRNA | Comparison | Expression Profile | miRDB predicted Targets of mature sequences |
|---|---|---|---|
| miR3150a | EpCAM(+)/CD133(+) vs. EpCAM(-)/CD133(-) | Downregulated (5p) | http://mirdb.org/cgi-bin/search.cgi?searchType=miRNA&full=mirbase&searchBox=MIMAT0019206 |
| miR3653 | Orai1-OE EpCAM(+)/CD133(+) vs. Plasmid-only EpCAM(+)/CD133(+) | Upregulated (3p) | http://www.targetscan.org/cgi-bin/targetscan/vert_71/targetscan.cgi?mirg=hsa-miR-3653-3p<br><br>*Recently withdrawn from miRDB |
| | STIM1-OE EpCAM(+)/CD133(+) vs. Plasmid-only EpCAM(+)/CD133(+) | | |

## Figure 3

Phylogenetic analysis of HBV Region 1 for miRNAs expressed differentially in Huh-7 HCC CSCs. A) The Minimum Spanning Tree (MST) and B) the Minimum Evolution Tree (MET) for the miRNAs and Region 1 of different HBV genotypes. In MST, the HBV genotypes (orange) and the miRNAs found close to HBV Region 1 both in MST and MET (blue) are shown. C) Expression profiles and target details of the miRNAs found close to HBV region 1 in MST and MET. None of the miRNAs listed are changed upon plasmid-only transfection.

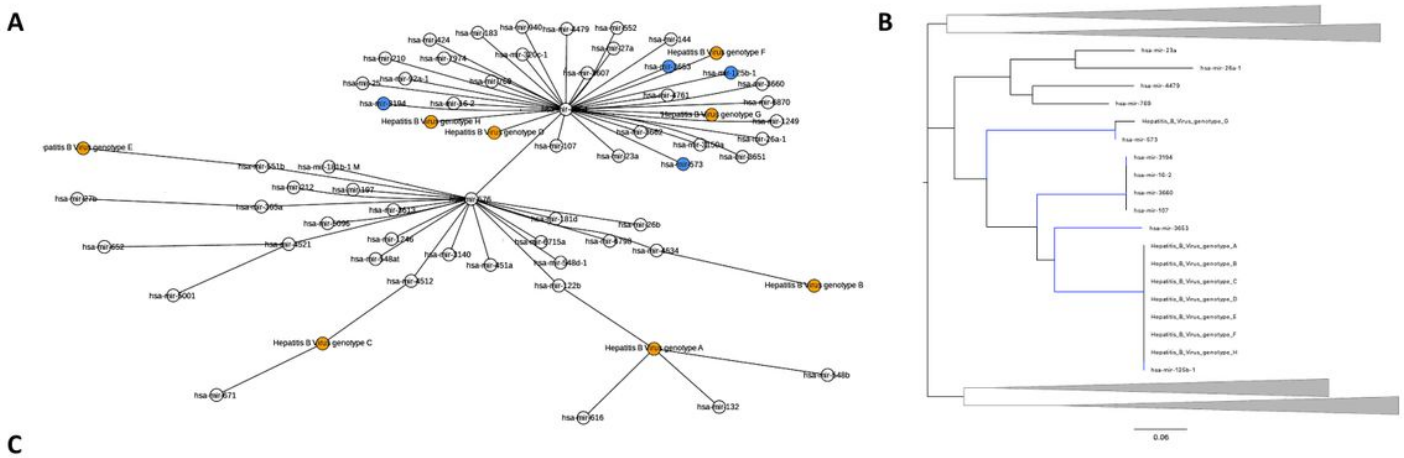


C

| miRNA | Comparison | Expression Profile | miRDB predicted targets of mature sequences |
|---|---|---|---|
| miR125b-1 | EpCAM(+)/CD133(+) vs. EpCAM(-)/CD133(-) | Downregulated (3p) | http://mirdb.org/cgi-bin/search.cgi?searchType=miRNA&full=mirbase&searchBox=MIMAT0004592 |
| miR3653 | Orai1-OE EpCAM(+)/CD133(+) vs. Plasmid-only EpCAM(+)/CD133(+)<br>STIM1-OE EpCAM(+)/CD133(+) vs. Plasmid-only EpCAM(+)/CD133(+) | Upregulated (3p) | http://www.targetscan.org/cgi-bin/targetscan/vert_71/targetscan.cgi?mirg=hsa-miR-3653-3p<br>*Recently withdrawn from miRDB |
| miR3194 | EpCAM(+)/CD133(+) vs. EpCAM(-)/CD133(-) | Upregulated (5p) | http://mirdb.org/cgi-bin/search.cgi?searchType=miRNA&full=mirbase&searchBox=MIMAT0015078 |

## Figure 4

Phylogenetic analysis of HBV Region 2 for miRNAs expressed differentially in Huh-7 HCC CSCs. A) The Minimum Spanning Tree (MST) and B) the Minimum Evolution Tree (MET) for the miRNAs and Region 2 of different HBV genotypes. In MST: the HBV genotypes (orange) and the miRNAs found close to HBV Region 2 both in MST and MET (blue) are shown. C) The expression profiles and the target details of the miRNAs found close to HBV region 2 in MST and MET.

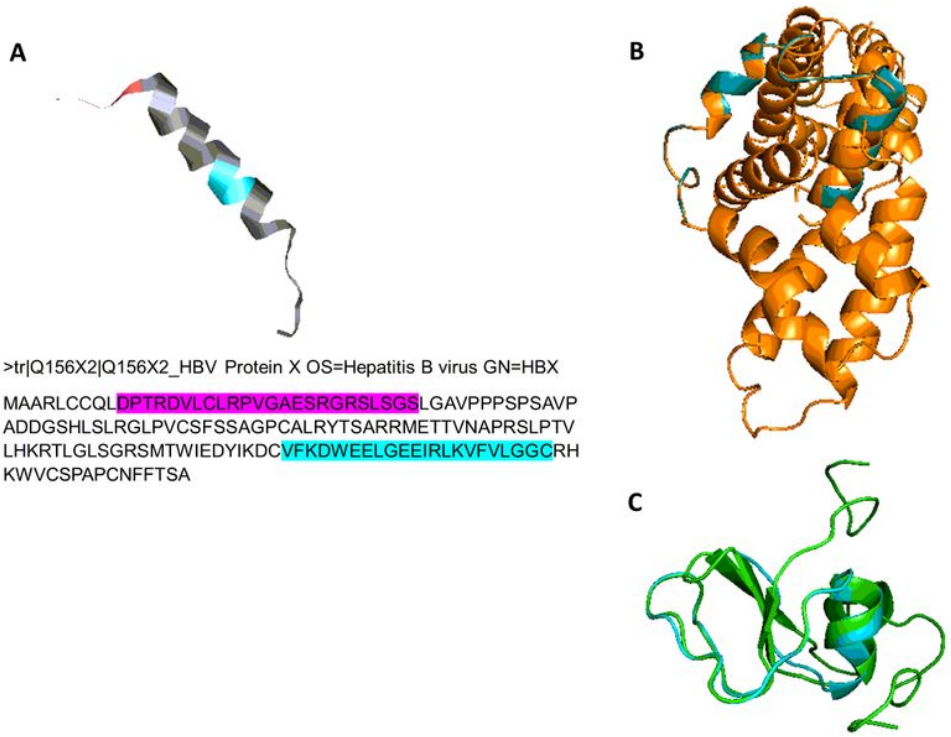


## Figure 5

Ribbon diagram for a putative protein encoded by regions 1 and 2 on HBx protein and homology analysis results for HBV Region 2. A) Region 1 (Pink) (from HBV amino acid 469 to 490; HBx amino acid 10-34) and Region 2 (cyan) (from HBV amino acid 574 to 590; HBx amino acid 117-138) on HBx protein. Superimposed homologies for B) 3lra.1.A structure, Mpp7 (orange), where this heterodimer contains 13 α-helix and Region 2 for HBV genotypes A, B, E, G and H, and C) 1ksq.1.A structure, Latent Transforming Growth Factor β-Binding Protein 1, TGFβ-LTBP-1 (green), showing a monomeric core structure with two α-helices covered by three β-sheets, and Region 2 of HBV genotypes C, D and F (cyan).

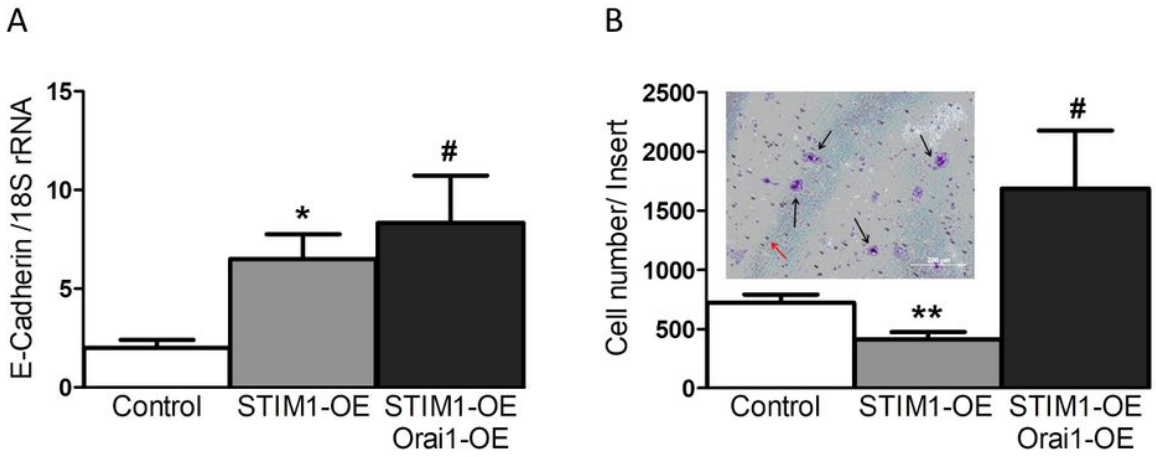


## Figure 6

Functional analyses on STIM1- and/or Orai1-enhanced Huh-7 HCC CSCs. A) E-Cadherin mRNA expression after enhancement of STIM1 and/or Orai1. E-Cadherin transcription levels were normalized to 18S rRNA levels (Target gene/18S rRNA mRNA x 102, * $p<0.05$, control vs. STIM1-OE; # $p<0.05$, control vs. STIM1- & Orai1-OE; Student's t test, unpaired, n=4). Control: transfected with plasmid (PCMV6) only, OE: overexpression. B) Invasion characteristics of STIM1-OE or STIM1&Orai1-OE Huh-7 HCC CSCs. ** $p<0.01$, control vs. STIM1-OE; # $p<0.05$, STIM1-OE vs. STIM1- & Orai1-OE; Student's t test, unpaired, n=8). Insert: Microscopic image of Huh-7 HCC CSCs run on invasion assay. Black arrows show cells (purple) that crossed 0.8-micrometer-diameter pores (red arrow) on matrigel membrane-containing well inserts. (Scale bar, 200 µm, marker 10x objective, Olympus IX71).

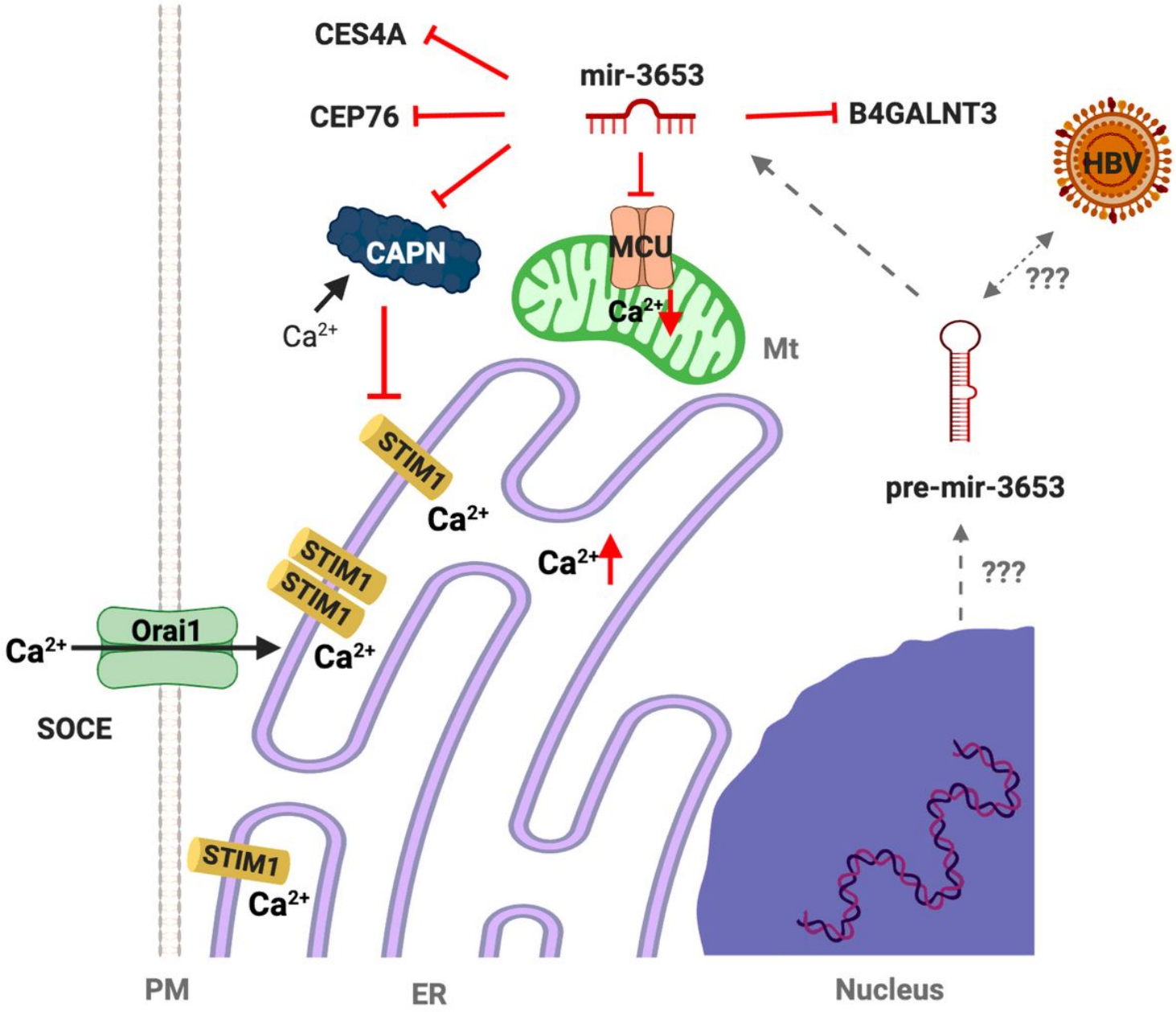


## Figure 7

A schematic description of a possible deception of host defense system by miR3653 in STIM1- and/or Orai1-enhanced Huh-7 HCC CSCs. CAPN: Calpain, a STIM-degrading Ca2+-dependent protease (downregulated); MCU: Mitochondrial Ca2+ uniporter (downregulated); STIM1: ER Ca2+ sensor (upregulated); SOCE “Store-operated Ca2+ entry” (upregulated by enhancement of both STIM1 and Orai1). Ca2+ uptake into ER by SERCA (sarcoplasmic-endeplasmic Ca2+-ATPase) is not shown for

simplicity. End result: cell survival, escape from apotosis, suppressed invasion. (Created with using BioRender)

## Supplementary Files

This is a list of supplementary files associated with this preprint. Click to download.

- SupplementaryTable4.docx
- SupplementaryTable3.docx
- SupplementaryTable2.docx
- SupplementaryTable1.docx